

# Round-robin measurements of the laser-induced damage threshold with sub-picosecond pulses on optical single layers

Laurent Lamaignère<sup>Ⓛ</sup>,<sup>a,\*</sup> Alexandre Ollé,<sup>a</sup> Marine Chorel<sup>Ⓛ</sup>,<sup>a</sup>  
Nadja Roquin,<sup>a</sup> Alexei A. Kozlov<sup>Ⓛ</sup>,<sup>b</sup> Brittany N. Hoffman<sup>Ⓛ</sup>,<sup>b</sup>  
James B. Oliver,<sup>b</sup> Stavros G. Demos,<sup>b</sup> Laurent Gallais,<sup>c</sup>  
Raluca A. Negres<sup>Ⓛ</sup>,<sup>d</sup> and Andrius Melninkaitis<sup>e</sup>

<sup>a</sup>CEA, CESTA, F-33116 Le Barp, France

<sup>b</sup>University of Rochester, Laboratory for Laser Energetics, Rochester, New York, United States

<sup>c</sup>Aix-Marseille University, CNRS, Centrale Marseille, Institut Fresnel, Marseille, France

<sup>d</sup>NIF and Photon Sciences, Lawrence Livermore National Laboratory, Livermore, California, United States

<sup>e</sup>Vilnius University, Laser Research Center, Vilnius, Lithuania

**Abstract.** The standardization and comparison of laser-damage protocols and results are essential prerequisites for development and quality control of large optical components used in high-power laser facilities. To this end, the laser-induced-damage thresholds of two different coatings were measured in a round-robin experiment involving five well-equipped damage testing facilities. Investigations were conducted at the wavelength of 1  $\mu\text{m}$  in the sub picosecond pulse duration range with different configurations in terms of polarization, angle of incidence, and environment (air versus vacuum). In this temporal regime, the damage threshold is known to be deterministic, i.e., the continuous probability distribution transitions from 0 to 1 over a very narrow fluence range. This in turn implies that the damage threshold can be measured very precisely. These characteristics enable direct comparison of damage-threshold measurements between different facilities, with the difference in the measured values indicating systematic errors or other parameters that were not previously appreciated. The results of this work illustrate the challenges associated with accurately determining the damage threshold in the short-pulse regime. Specifically, the results of this round-robin damage-testing effort exhibited significant differences between facilities. The factors to be taken into account when comparing the results obtained with different test facilities are discussed: temporal and spatial profiles, environment, damage detection, sample homogeneity, and nonlinear beam propagation. © 2020 Society of Photo-Optical Instrumentation Engineers (SPIE) [DOI: [10.1117/1.OE.60.3.031005](https://doi.org/10.1117/1.OE.60.3.031005)]

**Keywords:** laser damage; sub-picosecond pulses; coating; single layer; round-robin; damage threshold.

Paper 20200880SS received Jul. 23, 2020; accepted for publication Nov. 2, 2020; published online Nov. 21, 2020.

## 1 Introduction

The increase in energy and/or power of short-pulse-class lasers (OMEGA-EP,<sup>1</sup> PETAL,<sup>2</sup> and ARC<sup>3</sup>) in the picosecond regime requires components always more resistant to laser intensities, whether these are the compression gratings<sup>4</sup> or the mirrors that transport the beams to the target.<sup>5,6</sup> As a result, dedicated damage-testing facilities have been developed to provide an accurate determination of a component's ability to withstand the operational laser fluence. The question of the representativeness of the laboratory measurement arises logically in relation to the behavior of the components in real operational conditions. The environmental conditions are often not exactly the same, whereas the characteristics of the beams are somewhat different. But before even dealing with the representativeness of the measurement, it is just as relevant

---

\*Address all correspondence to Laurent Lamaignère, [laurent.lamaignere@cea.fr](mailto:laurent.lamaignere@cea.fr)

to question the reproducibility of tests carried out on different setups. Reproducibility in this instance is based on comparing measurements performed according to nominally the same protocol but on different facilities. *De facto*, the latter can differ in many respects, the characteristics of the laser beams are unavoidably not identical, and the diagnostics used for performing metrology are also different. Finally, the environmental conditions can also vary, and, in the end, the data processing may likewise prove to have some influence on the results to be compared. It is therefore important to consider how these differences can give rise to variations in the experimental results obtained at the different installations.

In the pulse regime reported in this work (sub-picosecond), it is well documented that the damage threshold for dielectric materials in pristine areas (free from obvious defects, such as micro-scale coating defects) is deterministic. This is reported in several previous works.<sup>7-10</sup> This is characterized by a very definite threshold behavior (deterministic), namely, that below a threshold value of energy density, the components are resistant to the laser flux, whereas above the threshold the damage is certain. This threshold can then be determined with great precision (the damage threshold is confined within a narrow range of fluences), and this behavior is well suited to the aim of this study, i.e., comparison of results obtained from different laboratories. Damage is associated with electronic processes, and it is closely linked to the properties of materials, in particular, their optical band gap and defect concentration. It turns out therefore that the damage threshold can even be predicted theoretically knowing the properties of the materials and those of the laser pulse.<sup>11-13</sup>

The objective of the work reported herein consists of comparing results of laser-induced-damage-threshold (LIDT) testing on two dielectric materials, HfO<sub>2</sub> and SiO<sub>2</sub>, in the form of single layers tested on five different laser facilities. The facilities have very similar characteristics such as similar wavelengths (around 1 μm), pulse duration (0.8 ps), and beam size. The tests were based on the protocol described by the ISO.<sup>14</sup> After the presentation of the raw results of LIDT measurements obtained using the various installations, the second part of the paper endeavors to identify and then analyze the various parameters, which are hypothesized to be the sources for the observed discrepancies between these measurements.

## 2 Results

### 2.1 Materials

Hafnia (HfO<sub>2</sub>) and silica (SiO<sub>2</sub>) single layers were selected for these tests as they are common materials used in multilayer dielectric optical components employed in short-pulse laser systems as high- and low-refractive-index materials, respectively. They have been deposited by electron-beam evaporation with ion assistance deposition on BK7 substrates. The layer thicknesses are 149.9 and 194.3 nm, respectively, with refractive indices of 1.930 and 1.448 determined at 1053 nm via ellipsometry. Multiple samples from the same deposition batch were fabricated and sent individually to the five testing facilities. This means that each test was carried out on a single sample, which should be nominally identical to all other samples in the batch. However, this equivalence assumption has not been verified by means of cross measurements. Therefore sample-to-sample repeatability will also be taken into account in the final comparison.

### 2.2 Experimental Conditions

The experimental conditions have been selected to be as close as possible between the different setups.

- a. Wavelength around 1 μm: 1053 or 1030 nm as a function of the laser source.
- b. Pulselength: around 800 fs, this value being quite common to the different lasers. The pulselengths were estimated from autocorrelator traces.
- c. Environment: in air due to the fact that only two setups are equipped with a vacuum chamber. Some tests have also been performed in a vacuum environment for comparison.
- d. Angle of incidence (AOI): 0° and 45°.
- e. Polarization: P and S polarizations.

The four testing configurations ( $0^\circ$ -P<sub>pol</sub>,  $45^\circ$ -P<sub>pol</sub>,  $0^\circ$ -S<sub>pol</sub>, and  $45^\circ$ -S<sub>pol</sub>) were implemented on the basis of the ISO 1-on-1 procedure on each setup.<sup>14</sup> Because damage in the sub-picosecond regime is deterministic, there is no need to perform a detailed statistical analysis by reproducing the measurement on a large number of spots per fluence. Finally, each laboratory had selected itself the number of sites and the fluence interval to minimize the sharp transition from 0% to 100% damage probability. The reported experimental LIDT (LIDT<sub>exp</sub>) is defined as the mean between the lowest fluence where damage is detected and the highest fluence where no damage occurs. The uncertainty of the measurement is set to be the mean absolute deviation between these two fluences. Therefore, the uncertainty of the measurement can be reduced by testing additional fluences around the damage-threshold fluence: to this end the fluence steps are decreased near the threshold.

The spatial profile of the laser-beam intensity was nearly Gaussian for all lasers used in this study. The equivalent areas are in the range ( $0.4 \times 10^{-4}$  to  $3.5 \times 10^{-4}$  cm<sup>2</sup>), which corresponds to beam diameters in the range (70 to 210 μm). The *in situ* damage detection was done either (a) analyzing the variation of the scattered light from the focal spot (damage is recorded when the scattered light increases, based on Schlieren imaging, see Fig. 1 of Ref. 15) or (b) direct imaging using a long-working distance microscope. However, these *in situ* detection approaches were used only for guidance during the 1-on-1 procedure and not as a damage threshold determination. The final determination was a precise observation with a differential-interferential-contrast (DIC) microscope, as recommended by the ISO standard. A damage site is defined as a modification, e.g., pits or discoloration, on the sample seen by means of the DIC. The results reported in this paper obtained from different facilities are presented anonymously in the form Lab A, B, C, D, and E (for laboratory A, B, C, D, and E).

### 2.3 Experimental Laser-Induced Damage Threshold

The experimental results of LIDTs obtained by the five laboratories on the two single layers and for the four configurations are given in Table 1. They are expressed in energy density (fluence in J cm<sup>-2</sup>), and reported based on the beam normal, that is to say that the beam area on the layers is not corrected for the AOI. The LIDTs are raw, as-measured data without taking into account the electric-field intensity (EFI) inside the single layer, which is different for each configuration.

**Table 1** LIDT<sub>exp</sub> measured by the five laboratories (labeled as Lab A, Lab B, Lab C, Lab D, and Lab E) on the two dielectric single layers (SiO<sub>2</sub> and HfO<sub>2</sub>). All values represent beam normal fluences in J cm<sup>-2</sup>. Results are also reported by lab C and lab E in a vacuum environment. “NLT Max Fluence” means that fluences necessary to perform the test cannot be reached (limit at 5 J cm<sup>-2</sup>). “—” means that the test was not realized.

	SiO <sub>2</sub> single layer				HfO <sub>2</sub> single layer			
	P-pol		S-pol		P-pol		S-pol	
	0°	45°	0°	45°	0°	45°	0°	45°
Lab A	4.15	5.07	—	5.11	3.40	4.67	—	5.24
Lab B	4.23	NLT Max Fluence	4.42	NLT Max Fluence	3.90	4.44	3.98	NLT Max Fluence
Lab C (air)	2.86	3.81	2.87	3.73	2.82	3.24	2.59	3.65
Lab C (vacuum)	3.44	4.18	3.09	4.77	3.19	3.83	2.85	4.35
Lab D	2.90	3.86	—	3.92	2.98	3.30	—	4.31
Lab E (air)	—	—	—	—	3.00	3.50	—	3.99
Lab E (vacuum)	—	—	—	—	—	4.25	—	4.75

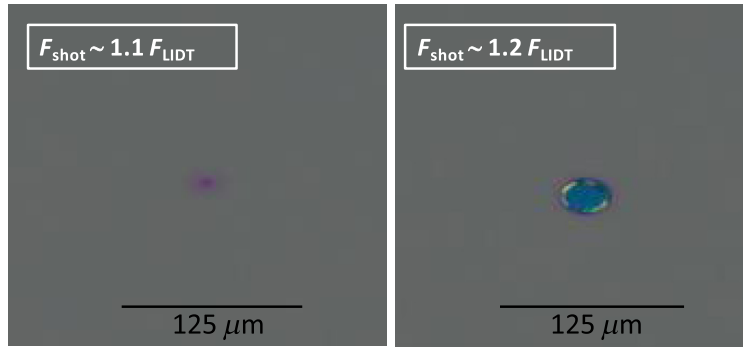


**Fig. 1** Post-mortem observation by means of a Nomarski microscope for two irradiations on HfO<sub>2</sub> at 10% and 20% above LIDT<sub>exp</sub>.

For illustration purposes, Fig. 1 shows two representative damage sites on HfO<sub>2</sub> irradiated at 10% and 20% above damage threshold, respectively, with the former being a light discoloration and the latter is a pit.

### 3 Discussion

#### 3.1 Electric Field Intensity

We base our discussion on the first-order assumption that each dielectric material is characterized by its own damage threshold. It is a property that is specific to it and other properties such as the melting temperature, the conductivity, and the permittivity. A material is thus characterized by its intrinsic LIDT (LIDT<sub>int</sub>), a property of the material independent of experimental conditions such as the AOI and the state of polarization of the beam. These last two parameters act on the maximum value of the EFI and on its position within the material (see Fig. 2). Thus intrinsic threshold and experimental threshold for a given layer are related by the EFI via the relationship:

$$\text{LIDT}_{\text{int}} = \text{LIDT}_{\text{exp}} \times \text{EFI}_{\text{max}}. \tag{1}$$

This implies that independent of the experimental conditions (AOI and polarization states), the LIDT<sub>int</sub> must be the same despite different LIDT<sub>exp</sub>. This property is beneficial and more essential to the damage metrology because it makes it possible:

- a. To compare results obtained under different experimental conditions.
- b. To check on the repeatability of a measurement on the same installation.
- c. To validate the accuracy of a measurement under uncertain experimental conditions, such as the occurrence of nonlinear effects (see for instance Sec. 3.2).

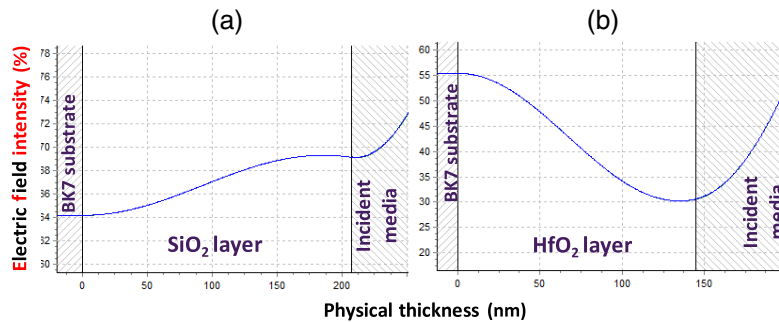


**Fig. 2** Electric field calculations in (a) SiO<sub>2</sub> and (b) HfO<sub>2</sub> single layers at 0° of AOI, P or S polarizations. The EFI is maximum at the top of the SiO<sub>2</sub> layer (at the air interface and its value is 69.9%) and maximum at the bottom of the HfO<sub>2</sub> layer (at the substrate interface and its value is 54.6%).

**Table 2** Calculated  $\text{EFI}_{\text{max}}$  in  $\text{SiO}_2$  and  $\text{HfO}_2$  single layers at  $0^\circ$  and  $45^\circ$  in P and S polarizations.

	P-pol		S-pol	
	$0^\circ$	$45^\circ$	$0^\circ$	$45^\circ$
$\text{SiO}_2 : \text{EFI}_{\text{max}}$	0.699	0.565	0.699	0.549
$\text{HfO}_2 : \text{EFI}_{\text{max}}$	0.546	0.422	0.546	0.372

Values of the refractive index and thickness were used to calculate numerically the EFI distribution within each single layer using OptiLayer software.<sup>16</sup> Samples are modeled as a single layer deposited on a semi-infinite BK7 substrate and a superstrate with a refractive index of 1 (air or vacuum). Samples are illuminated at normal incidence or  $45^\circ$  AOI, from the incident medium with a linearly polarized plane wave (horizontally or vertically) at the wavelength  $\lambda = 1053$  nm. The distribution of the square of the time-averaged electric field  $|E|^2$  is calculated and normalized by the incident electric field  $|E_{\text{inc}}|^2$ . The maximum enhancement of the EFI in the layer,  $|E|^2/|E_{\text{inc}}|^2$  denoted by  $\text{EFI}_{\text{max}}$  is estimated and given in Table 2 for the four configurations and the two single layers.

$$\text{EFI} = \left| \frac{E}{E_{\text{inc}}} \right|^2. \quad (2)$$

EFI calculations have also been made at the wavelength  $\lambda = 1030$  nm. Deviations between the EFIs at 1053 and 1030 nm are about 0.03% and 0.17% for  $\text{SiO}_2$  and  $\text{HfO}_2$  single layers, respectively. More the uncertainty in this factor using some nominal variances for the refractive index, the layer thickness, and the AOI were precisely discussed in Ref. 17. The uncertainties have been estimated about few %.

### 3.2 Intrinsic Laser-Induced Damage Threshold

The  $\text{LIDT}_{\text{int}}$  for the two single layers was estimated from Eq. (1) using the  $\text{LIDT}_{\text{exp}}$  values provided in Table 1 and calculated  $\text{EFI}_{\text{max}}$  given in Table 2. Results are given in Tables 3 and 4 for  $\text{SiO}_2$  and  $\text{HfO}_2$  single layers, respectively. For a meaningful comparison, only results obtained in air environment are reported. The last three columns of the tables indicate the average fluences measured on each installation as well as the standard deviation on the measurement.

**Table 3**  $\text{LIDT}_{\text{int}}$  of  $\text{SiO}_2$  single layer estimated by means of relation (1) from experimental data of Table 2 and  $\text{EFI}_{\text{max}}$  of Table 3. Thresholds are given in terms of energy density (fluence) in  $\text{J cm}^{-2}$ .

	$\text{SiO}_2$ monolayer						
	P-pol		S-pol		$\text{LIDT}_{\text{int}}$		
	$0^\circ$	$45^\circ$	$0^\circ$	$45^\circ$	mean	$\sigma$	$\sigma/\text{mean}$
Lab A	3.03	2.99	-	2.93	2.99	0.03	0.010
Lab B	2.96	NLT Max Fluence	3,09	NLT Max Fluence	3.02	0.07	0.023
Lab C	2.00	2.15	2.01	2.05	2.05	0.04	0.019
Lab D	2.03	2.18	—	2.15	2.12	0.05	0.023
Mean					2.55	0.53	0.209

**Table 4** LIDT<sub>int</sub> of HfO<sub>2</sub> single layer estimated by means of relation (1) from experimental data of Table 2 and EFL<sub>max</sub> of Table 3. Thresholds are given in terms of energy density (fluence) in J cm<sup>-2</sup>.

	HfO <sub>2</sub> monolayer						LIDT <sub>int</sub>	
	P-pol		S-pol		Mean	$\sigma$		$\sigma/\text{mean}$
	0°	45°	0°	45°				
Lab A	1.94	2.06	—	2.04	2.01	0.04	0.020	
Lab B	2.13	1.87	2.17	NLT Max Fluence	2.06	0.09	0.044	
Lab C	1.54	1.37	1.41	1.36	1.42	0.04	0.028	
Lab D	1.63	1.39	—	1.6	1.54	0.07	0.045	
Lab E	1.64	1.48	—	1.48	1.53	0.09	0.059	
Mean			—		1.71	0.30	0.175	

The standard deviation is a qualitative indicator of the repeatability of the measurement. The last line corresponds to the average of the measurements made on each installation.

To better visualize the distribution of the LIDT values obtained from measurements in the five different facilities, the results are also presented in the form of a histogram (Fig. 3). To quantify this distribution, the ratio between standard deviation and mean ( $\sigma/\text{mean}$ ) is used to estimate the deviation of the measurement. A number of behaviors can be readily appreciated.

- Globally, data are significantly dispersed (Fig. 3).
- Within each lab, the repeatability is about a few percent (lower than 7.5%, last column of Tables 3 and 4).
- The reproducibility (agreement between the results of measurements of the same measurand in the same configuration carried out with the same methodology between the five laboratories) is around 21% (last cell in Tables 3 and 4). This value is very large even if the error budgets of each installation are not taken into account at first analysis. Given that the experimental conditions are very similar and the fact that particular attention was paid to metrology during these tests to accurately determine the onset of damage, this difference between the LIDT maximum and minimum values (38%) is absolutely unexpected and highly undesirable. We will attempt in the next sections to provide insight into the possible underlying mechanisms.

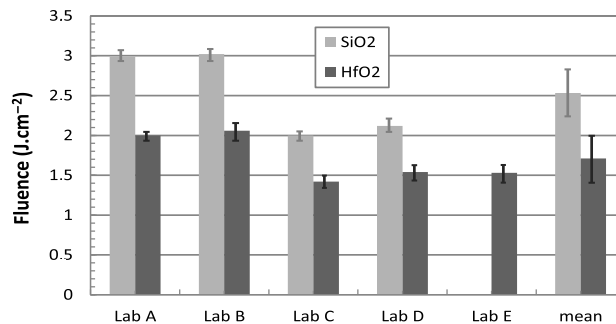


**Fig. 3** Histogram of intrinsic LIDTs on each laboratory for SiO<sub>2</sub> and HfO<sub>2</sub> single layers. The last two bars correspond to the averages of the different installations. Vertical lines are error bars.

### 3.3 Characteristics of the Laser Pulses

The tests were carried out at a pulse duration ( $\tau$ ) of 800 fs to achieve nominally identical conditions at the five laboratories regarding this parameter. The small deviations in this value were corrected using the temporal scaling law reported by Mero et al.,<sup>8</sup> in the form of  $F_{th} \sim \tau^\kappa$  with an exponent  $\kappa$  of about 0.30 and 0.33 for HfO<sub>2</sub> and SiO<sub>2</sub>, respectively.  $F_{th}$  stands for LIDT.

The pulse durations in all cases were estimated from the autocorrelation trace, but that estimation strongly depends on the assumption made on the shape of the temporal pulse (Gaussian, hyperbolic secant, and Lorentzian). The uncertainty on this measurement has also to be considered. On the other hand, the exact intensity profile must also be considered. Recently, Olle et al.<sup>13</sup> have reported experimentally and numerically large LIDT differences due to small differences in relatively similar intensity profiles (see Fig. 15 of Ref. 13). Ideally, exact temporal profiles have to be determined by means of specific apparatus such as frequency-resolved optical gating,<sup>18</sup> SPIRITED,<sup>19</sup> or other equivalent diagnostics. Finally, LIDT errors due to the pulse duration are certainly at least of the order of 5% but can also reach 30% for different intensity profiles. For this, we refer to Sec. 3 of Olle's article<sup>13</sup> dealing with the influence of temporal shape on the temporal scaling law.

Numerical LIDT<sub>int</sub> estimations based on the model described in Ref. 13 and based on the resolution of the multiple rate equation were also performed for three different temporal profiles acquired during this campaign at Lab B, by means of SPIRITED diagnostic. Small differences appear on their shapes and their full-width half maximum (FWHM) pulse durations are close (FWHM: 782 – 801 – 810 fs), see Fig. 4. Table 5 gives the LIDT<sub>int</sub> numerical estimations for SiO<sub>2</sub> and HfO<sub>2</sub>. Deviations between maximum and minimum values are about 9% and 5% for SiO<sub>2</sub> and HfO<sub>2</sub>, respectively. These deviations are part of the repeatability of the measurement on the same setup.

Another parameter that may have a significant impact is the temporal contrast. Prepulses and/or postpulses can have a double effect. First, it is established that the ablation efficiency in dielectrics depends on the delay between the pre-/post-pulses and the main pulse.<sup>20</sup> The first pulse promote electrons into the conduction band while the second pulse induces the ablation of

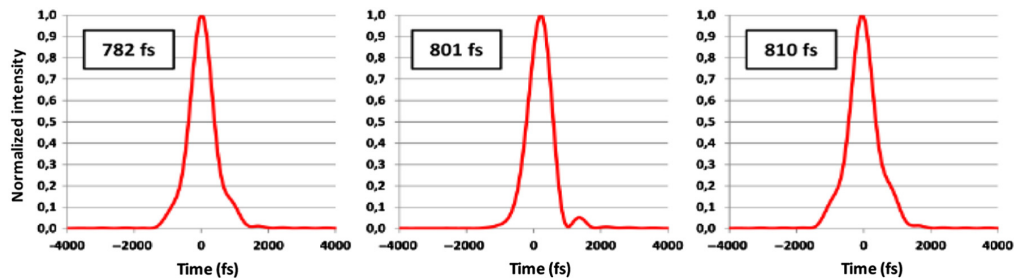


**Fig. 4** Three different temporal profiles measured during the campaign at Lab B by means of SPIRITED diagnostic, for the same laser fluence.

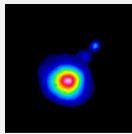
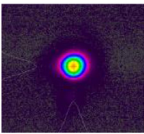
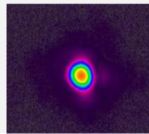
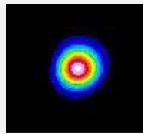
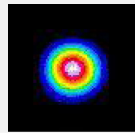
**Table 5** Numerical LIDTs ( $\text{J cm}^{-2}$ ) of SiO<sub>2</sub> and HfO<sub>2</sub> single layers estimated from numerical model for the three temporal profiles given in Fig. 4. Relation (1) can be applied to estimate the intrinsic LIDT.

	Pulse duration (fs)			mean	$\sigma$	$\sigma/\text{mean}$	$(\text{max} - \text{min})/\sigma$
	782	801	810				
SiO <sub>2</sub>	4.94	4.67	5.11	4.91	0.22	0.05	0.09
HfO <sub>2</sub>	4.47	4.36	4.59	4.47	0.12	0.03	0.05

the dielectric. The analogy with laser damage mechanisms is obvious. These pre- and post-pulses must be minimal and sufficiently spaced in time from the main pulse to avoid any pre- or post-excitation effect. In addition, these pulses are taken into account in the energy balance (the measurement of the pulse energy is integrated on a pyroelectric detector or on a photoelectric cell), biasing the true value of the intensity/energy involved in the process and damage mechanisms by the main pulse. The impact of this parameter is currently not known. Therefore, it may be important to include in the diagnostics the capability to measure the full intensity profile (for that purpose see Fig. 4 of Ref. 13).

The determination of beam fluence has been the gold standard in damage testing for decades. Its accuracy is intimately linked to a precise and rigorous determination of the equivalent beam area (Fig. 5). However, it can be challenging to ensure that the measurement is correct to better than 5%,<sup>15</sup> and the measure can strongly diverge via seemingly minor effects. Here, we detail a few missteps to be aware of when managing short pulses and small beams.

- a. The waist position and length: lenses with short focal lengths are commonly used on short-pulse damage setups to focus the laser beam on the sample to be tested and achieve damage threshold fluences. As a result, the Rayleigh length is also very short. The beam area is the same for only a few millimeters<sup>13</sup> and diverges strongly beyond. An approximate positioning of the sample and/or of the measurement camera can lead to a significant error on the beam area.
- b. The CCD sensor size versus ratio signal/noise: the pixel size of cameras commonly used to measure the beam profiles is only a few microns in length ( $\sim 5 \mu\text{m}$ ) and they are coded over 12-bit gradation or more. These two characteristics allow a high-quality resolution with corresponding accurate determination of the energy in the wings of the beam and a very good resolution of the maximum intensity of the same beam. However, the sensor size is large, of the order of 8 by 6 mm in comparison with the size of the beam ( $< 0.2 \text{ mm}$ ), that is to say a ratio close to 50. The total number of pixels on these sensors is around 2 million ( $1600 * 1200$ ) but the number of pixels illuminated for a beam of a hundred microns is only of the order of 2000, in this case, a ratio of 1000. Thus, the signal-to-noise ratio is strongly unfavorable for such small beams with such a large sensor. It is therefore advisable to adjust the size of the sensor to the size of the beam by imposing an adapted region of interest around the beam. In addition, cross-analysis between laboratories of the measurement of a given beam size has given a difference of at least 5%.
- c. Nonlinear beam propagation: operating with short pulses can lead to non-linear propagation inside transmissive optical components that are designed to facilitate energy control (waveplate and polarizer), focus the beam on the sample (lens), or split the beam to diagnostics (beamsplitter). This nonlinear propagation can modify the beam profile and its focal position. A beam size variation up to 5% has been reported by changing the pulse duration from 0.8 to 4 ps for a fixed beam energy (see Fig. 18 of Ref. 13). This could also be the case with the energy variation.

	Lab A	Lab B	Lab C	Lab D	Lab E
Beam diameter @ 1/e ( $\mu\text{m}$ )	$73 \pm 17$	$173 \pm 25$	$210 \pm 10$	$100 \pm 1$	$186 \pm 14$
Beam area @ 1/e ( $\text{cm}^2$ )	$(4.20 \pm 0.22) \times 10^{-5}$	$(2.36 \pm 0.05) \times 10^{-4}$	$(3.48 \pm 0.01) \times 10^{-4}$	$(7.85 \pm 0.01) \times 10^{-5}$	$(2.73 \pm 0.02) \times 10^{-4}$
Spatial profile					
Fluence determination	Maximum fluence of beam profile	Maximum fluence of beam profile			

**Fig. 5** Laser beam sizes and spatial for the five facilities.

- d. Operational environment: when laser-damage measurements of dielectric components are carried out, many questions arise as to the effect of the environment. This issue is quite complex, and it is not the purpose of this discussion to deal exhaustively with this topic. However, two issues are of particular interest. First, the effect of air in beam propagation, which can lead to air breakdown. Second, the change of the film properties (refractive index and layer thickness.) with the environment, potentially modifying the value of the EFI in the layer.

Self-focusing is known to be an important parameter for the design of short-pulse laser-damage setups, which is why it is recommended to carry out tests under a vacuum environment to circumvent this issue (with the difficulties inherent in measurements in a vacuum chamber). For tests in an air environment, it is necessary to estimate the B-integral through the focal volume prior to the test surface. In the setups, B-integral is due to the self-focusing in the air after the last focusing lens. For a Gaussian beam with a wavelength  $\lambda$  and waist radius  $\omega$ , the Rayleigh distance  $Z_R$  is defined as

$$Z_R = \pi \frac{\omega^2}{\lambda}. \quad (3)$$

The intensity  $I$  at the focal spot is given by the relation:

$$I = \frac{2 \cdot E}{\tau \pi \omega^2}, \quad (4)$$

where  $E$  is the energy and  $\tau$  the pulse duration. The B-integral can be estimated as

$$B = \frac{2\pi}{\lambda} n_2 \int_0^{Z_R} I(z) dz. \quad (5)$$

The intensity  $I$  is assumed to be constant within the Rayleigh distance  $Z_R$ , then combination of Eqs. (3)–(5) gives

$$B = \frac{4\pi}{\lambda^2} n_2 \frac{E}{\tau} \quad (6)$$

During all of the tests, samples were tested up to  $6 \text{ J cm}^{-2}$  in the beam normal at 800 fs. It has been established that the nonlinear refractive index of air was  $n_2 = 3.10 \cdot 10^{-19} \text{ cm}^2/\text{W}$ ,<sup>21</sup> it follows that Eq. (6), with an energy of 2 mJ, which corresponds to the maximum energy delivered during these tests, gives a B-integral value of  $B \sim 0.85$ . This value is below the self-focusing limit, which can be taken as  $B \sim 2 \text{ rad}$ .<sup>22</sup> Thus, beam propagation should not be subject to self-focusing.

This issue was also verified experimentally by changing the AOI from  $0^\circ$  to  $45^\circ$  and verifying that the  $\text{LIDT}_{\text{int}}$  estimated from the  $\text{LIDT}_{\text{exp}}$  remains constant. This is based on the following testing hypothesis: given that the test fluence increases when the AOI is increased, if the self-focusing effect is negligible one should find the same intrinsic LIDT for any AOI and corresponding fluence. The EFI was calculated at each AOI; it must be specified that the uncertainty on its determination increases with the AOI. Results are given in Table 6. Increasing the AOI

**Table 6**  $\text{LIDT}_{\text{int}}$  of  $\text{HfO}_2$  single layer estimated from  $\text{LIDT}_{\text{exp}}$  tested in air environment and S-polarization between  $0^\circ$  and  $45^\circ$  AOI during the campaign at Lab B. EFI was determined at each angle, the uncertainty (not reported here) on its estimation increases with the AOI.<sup>17</sup>

	$0^\circ$	$10^\circ$	$20^\circ$	$30^\circ$	$35^\circ$	$40^\circ$	$45^\circ$
$\text{LIDT}_{\text{exp}}$ ( $\text{J cm}^{-2}$ )	$3.77 \pm 0.07$	$3.75 \pm 0.01$	$4.15 \pm 0.08$	$4.50 \pm 0.06$	$4.70 \pm 0.10$	$5.08 \pm 0.01$	$5.57 \pm 0.01$
EFI	0.541	0.533	0.509	0.466	0.438	0.405	0.366
$\text{LIDT}_{\text{int}}$ ( $\text{J cm}^{-2}$ )	$2.04 \pm 0.07$	$2.00 \pm 0.01$	$2.11 \pm 0.08$	$2.10 \pm 0.06$	$2.06 \pm 0.10$	$2.06 \pm 0.01$	$2.08 \pm .001$

means an increase of the experimental fluence (from 3.77 to 5.57 J cm<sup>-2</sup> in the reported case for experiments carried out by Lab B). And yet, it is observed that the intrinsic LIDT is quite constant within experimental error, without the error in determining the EFI being taken into account. The mean value and the standard deviation are 2.06 and 0.02 J cm<sup>-2</sup>, respectively, which is a variation of <1%. It can be concluded that

- a. The intrinsic LIDT can be determined at any AOI, based on the calculated EFI.
- b. No self-focusing occurred during these measurements, even at high energy.

The question of the impact of the environment for testing is a difficult question. Specifically, can one extrapolate results from thresholds measured in the air to expected thresholds in vacuum? This is a complex question to which an element of an answer is brought indirectly in this paragraph. To explore this question, EFI values were estimated for the layers in vacuum. We start from the principle that the vacuum can be approximated by a dry air environment, in particular with regards to the refractive index of the dielectric layers. The estimation of the refractive index not being possible with our means in vacuum, measurements with a spectrophotometer in dry air were carried out to estimate the refractive index of the layers, and therefore determine the value of the EFI. Refractive indices, and consequently EFIs, were found to be little different regardless of the environment. Damage thresholds were subsequently measured in ambient air (45% relative humidity) and in dry air (4% relative humidity) on one HfO<sub>2</sub> single layer and one SiO<sub>2</sub> single layer. LIDT<sub>exp</sub> were also measured to be approximately the same. Finally, intrinsic LIDT values are quite similar (see Table 7), with differences of <3%. These results suggest that “intrinsically,” environment should have a negligible effect on the damage thresholds of these samples. A key aspect of this determination is the relatively slow change in EFI versus layer thickness for a single layer, such as those tested in this study, versus the very rapid change in EFI for some multilayer coating designs.<sup>23</sup> The EFI becomes much more complex when these materials are integrated in multilayer coating designs, requiring additional investigation beyond the scope of this work.

Despite this analysis, a significant difference was nevertheless obtained experimentally between tests carried out in air and in vacuum. Table 1 reports higher LIDT<sub>exp</sub> in vacuum than in air, these results were obtained by both Lab C and Lab E. For HfO<sub>2</sub> coating, LIDT<sub>int</sub> are 1.42 and 1.34 J cm<sup>-2</sup> in air and 1.63 and 1.52 J cm<sup>-2</sup> in vacuum, from laboratories C and E, respectively. This means a difference of around 13% for the two labs.

- e. Error budget: One can consider an exhaustive list of all sources of error leading to an approximate determination of the damage thresholds. However, the most important ones are arguably the following:
  1. Fluence is the most common quantity reported however is indirectly derived from energy and beam size measurements: The error on energy is only a few percent because the pyroelectric detectors are calibrated against a standard. Measuring the area of the beam is certainly one of the most delicate measurements. In a previous article comparing cameras, measurement plans, and correlations between different measurement

**Table 7** LIDT<sub>exp</sub> of HfO<sub>2</sub> and SiO<sub>2</sub> single layers measured in ambient and dry air, at 0° AOI during the campaign at Lab B. LIDT<sub>int</sub> were estimated with EFI calculated from refractive indices measured in ambient and air environments.

Dielectric monolayer	Environment	Refractive index at 1053 nm	Physical thickness of layer (nm)	EFI <sub>max</sub>	LIDT <sub>exp</sub> (J cm <sup>-2</sup> )	LIDT <sub>int</sub> (J cm <sup>-2</sup> )
HfO <sub>2</sub>	Ambient air	1.93	149.9	0.5414 ± 0.0160	3.90 ± 0.01	2.11 ± 0.01
	Dry air	1.96		0.5409 ± 0.0047	3.81 ± 0.04	2.06 ± 0.02
SiO <sub>2</sub>	Ambient air	1.448	149.3	0.6890 ± 0.0040	4.23 ± 0.15	2.91 ± 0.10
	Dry air	1.446		0.7012 ± 0.0099	4.07 ± 0.25	2.85 ± 0.17

means, it emerged that an absolute error of 10% is to be taken into account on this parameter.<sup>15</sup> Sozet<sup>24</sup> has also estimated an absolute error about 10% for laser damage tests carried out at 1053 nm to 0.7 fs on the DERIC facility taking into account the errors on beam-energy measurement and on equivalent-area determination.

2. Damage detection, even with the help of a microscope, is somewhat subjective. It is difficult to quantify its weight in the error budget. Sozet,<sup>25</sup> by comparing two measurement procedures, reported a difference of 5% linked to the criterion for determining the threshold.
3. Chores et al.<sup>17</sup> focused on the error in determining the intrinsic threshold, paying particular attention to the errors in the EFI based on uncertainties in the thicknesses and refractive indices of the layers. This makes it possible to give advice on reducing this uncertainty, for example by optimizing the AOI of the tests. We can refer to the article as a whole for more information. The correlation between the intrinsic LIDT and the AOIs should be further investigated in the future in order to strengthen the results reported in Table 6.
4. Pulse duration is estimated from the autocorrelation trace. Again, an error of the order of 10% is to be considered. But beyond that, a strong relationship emerges between the damage threshold and the true intensity profile,<sup>13</sup> the latter not being known and measured on a daily basis. Small differences in intensity profiles can result in large differences in thresholds. These differences must be taken into account on a case-by-case basis.
5. Within the context of the analysis provided in this work, we have assumed that the damage threshold under exposure to sub-ps pulses is not dependent of the size of the damage testing beam spot. This is considered to be valid as damage initiation tests the fundamental limits of the material and is not dependent on the density of a defect distribution (damage is initiated by electric-field-induced volume breakdown<sup>10</sup>). However, this might not be entirely correct. This difference can arise from energy balance considerations, namely that damage requires not only the deposition of energy to create volume breakdown conditions but also the energy to generate the observed material modifications. It is the latter component that may be sensitive to the area of the ablated volume (thus, the size of the damage testing beam). To the best of our knowledge, the potential role of this process in the measured damage threshold under exposure to sub-ps laser pulses has not been explored yet. However, there are publications that indicate a dependence of the ablation threshold of materials on the beam size.<sup>26–28</sup> Also, a recent work focused on the damage threshold in dielectric materials and coatings<sup>29</sup> seems to

**Table 8** Synthesis of error margins (standard uncertainty at  $1\sigma$ ) for identified contributors (error budget). A quadratic summation provides an accuracy around 19% for the determination of fluences.

Contributor	Error bar at $1\sigma$ (%)
1 Calorimeter	2
2 Beam size estimation	5
3 Damage detection	5
4 Pulse duration estimation and dependence	10
5 Beam size dependence	15
Total budget	37
Quadratic summation	19

indicate (see Fig. 5 of Ref. 29) that the damage threshold at pulse durations similar to those used in this work vary by up to about 15% for beam waists of 100, 50, and 30  $\mu\text{m}$ . Therefore, the size of the damage testing beam may be another parameter that can have an impact in the measured damage threshold and may require additional study.

Thus, considering the analysis of the impact of all of these different contributors (they are summarized in Table 8 with the assumption that they are not correlated), it is appropriate to consider that differences around 20% between tests carried out on different facilities can be reasonably obtained.

#### 4 Conclusion—Perspectives

The round robin conducted by five independent laboratories on LIDT measurements of two dielectric single layers in the short pulse regime at 1  $\mu$  and for four different experimental configurations showed significant differences. Deviations on average of around 21% were obtained greater than the absolute measurement uncertainties on the facilities estimated at least 10%. This is an unexpected and highly undesirable result. LIDT determination in this pulse-length regime should be straightforward and results should be comparable. However, an analysis of the various contributors involved in the measurement of damage thresholds shows that differences of 20% are nevertheless plausible. The hypothesized principal mechanism to explain such deviations needs to be explored in future work to resolve this challenge in determining damage-threshold measurements in the short pulse regime. We suggest that it is of fundamental importance to pay increased attention to metrology:

- a. Accurate beam spatial profile measurement with special attention to the sensor noise determination in the case of a small beam on a large sensor window.
- b. The problem of nonlinear beam propagation, which affects the experimental measurements, mainly the beam profile, has to be considered.
- c. Experimental conditions have to be perfectly known and controlled, as for example hygrometry and/or environment.
- d. Precise knowledge of the temporal intensity profile is also imperative.

#### Acknowledgments

This material is based in part upon work supported by the Department of Energy (DOE) National Nuclear Security Administration under Award No. DE-NA0003856, the University of Rochester, and the New York State Energy Research and Development Authority. This report was prepared as an account of work sponsored by an agency of the U.S. Government. Neither the U.S. Government nor any agency thereof, nor any of their employees, makes any warranty, express or implied, or assumes any legal liability or responsibility for the accuracy, completeness, or usefulness of any information, apparatus, product, or process disclosed, or represents that its use would not infringe privately owned rights. Reference herein to any specific commercial product, process, or service by trade name, trademark, manufacturer, or otherwise does not necessarily constitute or imply its endorsement, recommendation, or favoring by the U.S. Government or any agency thereof. The views and opinions of authors expressed herein do not necessarily state or reflect those of the U.S. Government or any agency thereof. Part of this work was performed under the auspices of the U.S. DOE by Lawrence Livermore National Laboratory under Contract No. DE-AC52-07NA27344.

#### References

1. L. J. Waxer et al., “High-energy petawatt capability for the OMEGA laser,” *Opt. Photonics News* **16**(7), 30–36 (2005).
2. N. Blanchot et al., “1.15 PW-850 J compressed beam demonstration using the PETAL facility,” *Opt. Express* **25**(15), 16957–16970 (2017).

3. J. E. Heebner et al., "Injection laser system for advanced radiographic capability using chirped pulse amplification on the National Ignition Facility," *Appl. Opt.* **58**, 8501 (2019).
4. J. Néauport et al., "Effect of electric field on laser induced damage threshold of multilayer dielectric gratings," *Opt. Express* **15**(19), 12508–12522 (2007).
5. R. A. Negres et al., "Laser-induced damage of intrinsic and extrinsic defects by picosecond pulses on multilayer dielectric coatings for petawatt-class lasers," *Opt. Eng.* **56**, 011008 (2017).
6. M. Chorel et al., "Robust optimization of the laser induced damage threshold of dielectric mirrors for high power lasers," *Opt. Express* **26**, 11764 (2018).
7. B. C. Stuart et al., "Laser-induced damage in dielectrics with nanosecond to subpicosecond pulses," *Phys. Rev. Lett.* **74**(12), 2248–2251 (1995).
8. M. Mero et al., "Scaling laws of femtosecond laser pulse induced breakdown in oxide films," *Phys. Rev. B* **71**, 115109 (2005).
9. B. Mangote et al., "A high accuracy femto-/picosecond laser damage test facility dedicated to the study of optical thin films," *Rev. Sci. Instrum.* **83**, 013109 (2012).
10. A. A. Kozlov et al., "Mechanisms of picoseconds laser-induced damage in common multilayer dielectric coatings," *Sci. Rep.* **9**(1), 607 (2019).
11. B. Rethfeld et al., "Interaction of dielectrics with femtosecond laser pulses: application of kinetic approach and multiple rate equation," *Appl. Phys. A* **101**, 19 (2010).
12. L. Gallais et al., "Wavelength dependence of femtosecond laser-induced damage threshold of optical materials," *J. Appl. Phys.* **117**, 223103 (2015).
13. A. Olle et al., "Implications of laser beam metrology on laser damage temporal scaling law for dielectric materials in the picosecond regime," *Rev. Sci. Instrum.* **90**, 073001 (2019).
14. ISO Standard Nos. 21254-1–21254-4 (2011).
15. L. Lamainère et al., "Parametric study of laser-induced surface damage density measurements: toward reproducibility," *J. Appl. Phys.* **107**, 023105 (2010).
16. A. V. Tikhonravov and M. K. Trubetskov, "OptiLayer thin film software," Optilayer Ltd., <http://www.optilayer.com>.
17. M. Chorel et al., "Influence of absorption-edge properties on subpicosecond intrinsic laser-damage threshold at 1053 nm in hafnia and silica monolayers," *Opt. Express* **27**, 16922 (2019).
18. R. Trebino, *Frequency-Resolved Optical Gating: The Measurement of Ultrashort Laser Pulses*, Kluwer Academic (2000).
19. D. Bigourd et al., "Direct spectral phase measurement with spectral interferometry resolved in time extra dimensional," *Rev. Sci. Instrum.* **81**, 053105 (2010).
20. K. Gaudfrin et al., "Fused silica ablation by double femtosecond laser pulses: influence of polarization state," *Opt. Express* **28**, 15189 (2020).
21. E. T. J. Nibbering et al., "Determination of the inertial contribution to the nonlinear refractive index of air, N<sub>2</sub> and O<sub>2</sub> by use of unfocused high-intensity femtosecond laser pulses," *J. Opt. Soc. Am. B* **14**, 650–660 (1997).
22. D. Villate, N. Blanchot, and C. Rouyer, "Beam breakup integral measurement on high-power laser chains," *Opt. Lett.* **32**, 524–526 (2007).
23. J. B. Oliver et al., "Optimization of laser-damage resistance of evaporated hafnia films at 351 nm," *Proc. SPIE* **7132**, 71320J (2008).
24. M. Sozet et al., "Laser damage density measurement of optical components in the subpicosecond regime," *Opt. Lett.* **40**, 2091 (2015).
25. M. Sozet et al., "Assessment of mono-shot measurement as a fast and accurate determination of the laser-induced damage threshold in the sub-picosecond regime," *Opt. Lett.* **41**, 804 (2016).
26. B. M. Kim et al., "Effects of high repetition rate and beam size on hard tissue damage due to subpicosecond laser pulses," *Appl. Phys. Lett.* **76**, 4001–4003 (2000).
27. S. Martin et al., "Spot-size dependence of the ablation threshold in dielectrics for femtosecond laser pulses," *Appl. Phys. A* **77**, 883–884 (2003).
28. A. Hertwig et al., "Interaction area dependence of the ablation threshold of ion-doped glass," *Thin Solid Films* **453–454**, 527–530 (2004).

29. T. A. Laurence et al., "Role of defects in laser-induced modifications of silica coatings and fused silica using picosecond pulses at 1053 nm: II. Scaling laws and the density of precursors," *Opt. Express* **25**, 15381–15401 (2017).

Biographies of the authors are not available.